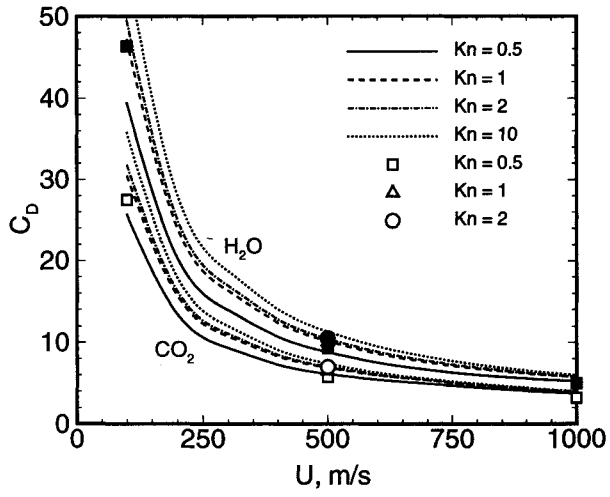

Fig. 3 $(C_D)_{ave}$ and $(C_D)_{DSMC}$ vs U for several values of Kn. The symbols are DSMC results: solid = H_2O, open = CO_2.

as the inverse of molecular weight, at a given U; hence, CO_2 has the lowest C_D, and H_2O the highest.

Figures 2 and 3 show that the agreement between $(C_D)_{DSMC}$ and $(C_D)_{ave}$ is quite good at velocities of 500 and 1000 m/s; however, at 100 m/s the agreement degrades slightly. $(C_D)_{ave}$ underpredicts $(C_D)_{DSMC}$ by up to 15% at U = 100 m/s, Kn = 0.5.

Drag in Multicomponent Gas Mixtures

The drag on a particle in a mixture of gases can be written as

$$D = \sum_i \frac{1}{2} \rho_i U^2 A C_{D_i} \tag{8}$$

where i represents the gas. The drag can be written in terms of mass fraction as

$$D = \frac{1}{2} \rho U^2 A \sum_i X_i C_{D_i} \tag{9}$$

to give the total drag on the particle in a mixture of gases. Thus, since the drag correlations represent the C_D of the individual plume gases, they can also be used in situations involving gas mixtures.

Conclusions

$(C_D)_{ave}$ gives good overall agreement with the $(C_D)_{DSMC}$ for CO, N_2, CO_2, and H_2O gases at representative solid rocket plume temperatures. Hence, $(C_D)_{ave}$ can be used in engineering applications to plumes. In applications in which it might not be feasible to use $(C_D)_{ave}$, the Hermsen drag correlation can be used since it is the most accurate of the four empirical correlations.

Acknowledgments

This research was performed under subcontracts A93S-9 and A94S-24 with Sverdrup Technology, Inc., Arnold Air Force Base, Tennessee, and monitored by Robert A. Reed and Robert S. Hiers, III. The authors wish to acknowledge the many helpful discussions about DSMC with Richard G. Wilmoth of NASA Langley Research Center, Hampton, Virginia.

References

[1]Vogenitz, F. W., Bird, G. A., Broadwell, J. E., and Rungaldier, H., "Theoretical and Experimental Study of Rarefied Supersonic Flows About Several Simple Shapes," *AIAA Journal*, Vol. 6, No. 12, 1968, pp. 2388–2394.

[2]Bird, G. A., "Monte-Carlo Simulation in an Engineering Context," *Rarefied Gas Dynamics*, edited by S. S. Fisher, Vol. 74, Pt. I, Progress in Astronautics and Aeronautics, AIAA, New York, 1981, pp. 239–255.

[3]Bird, G. A., *Molecular Gas Dynamics and the Direct Simulation of Gas Flows*, Oxford Sciences Publications, Clarendon, Oxford, England, UK, 1994.

[4]Bird, G. A., "The G2/A3 Program System Users Manual," G. A. B. Consulting Pty. Ltd., Version 1.8, Killara, New South Wales, Australia, March 1992.

[5]Hermsen, R. W., "Review of Particle Drag Models," JANNAF Performance Standardizations Subcommittee 12th Meeting Minutes, Chemical Propulsion Information Agency, Jan. 1979; also Nickerson, G. R., Coats, D. E., Hermsen, R. W., and Lamberty, J. T., Jr., "A Computer Program for the Prediction of Solid Propellant Rocket Motor Performance (SPP)," Air Force Rocket Propulsion Lab., AFRPL TR-83-036, Edwards AFB, CA, Sept. 1984, Section 6.3.

[6]Henderson, C. B., "Drag Coefficients of Spheres in Continuum and Rarefied Flows," *AIAA Journal*, Vol. 14, No. 6, 1976, pp. 707, 708.

[7]Crowe, C. T., "Drag Coefficient of Particles in a Rocket Nozzle," *AIAA Journal*, Vol. 5, No. 5, 1967, pp. 1021, 1022.

[8]Carlson, D. J., and Hoglund, R. F., "Particle Drag and Heat Transfer in Rocket Nozzles," *AIAA Journal*, Vol. 2, No. 11, 1964, pp. 1980–1984.

[9]Fields, J. C., "DSMC Analysis of Heat Transfer and Drag on Particles in Solid Rocket Plumes," M.S. Thesis, Dept. of Mechanical and Aerospace Engineering, Univ. of Missouri–Rolla, Rolla, MO, Dec. 1994.

Two-Parameter Wideband Spectral Model for the Absorption Coefficients of Molecular Gases

K. Kamiuto*
Oita University, Oita 870-11, Japan

Introduction

LOW-RESOLUTION spectral models for the absorption coefficients of IR gases are needed to perform efficient spectral computations of radiative transfer in real gases[1] or in gas-particle composite media.[2]

The Edwards model[1] and modified Edwards model[3] derived from the Elsasser regular band model with the exponential band-envelope have been utilized for this purpose. These models can be generally represented in the following form:

$$\kappa_\nu = (\alpha/K_1\omega)\exp[-\Delta\nu/K_1\omega]\tanh K_2\eta \tag{1}$$

Here, α is the integrated band intensity (cm^{-1}/gm^{-2}), ω is the bandwidth parameter (cm^{-1}), η is the line-overlap parameter, and K_1 and K_2 are the parameters. Furthermore, $\Delta\nu$ is defined as follows: $\Delta\nu = \nu_u - \nu$, for an asymmetric band with upper limit ν_u, $\Delta\nu = \nu - \nu_l$, for an asymmetric band with lower limit ν_l, and $\Delta\nu = 2|\nu - \nu_c|$, for a symmetric band with center ν_c. In the expression for $\Delta\nu$, ν is the wave number of radiation (cm^{-1}).

Received Aug. 15, 1994; revision received Nov. 8, 1994; accepted for publication Dec. 19, 1994.

*Professor, High-Temperature Heat Transfer Laboratory, Department of Production Systems Engineering. Member AIAA.

Table 1 Obtained values of K_1 and K_2

	Pressure, bar				
	Total	Partial	K_1	K_2	Standard deviation, σ^*
CO_2	0.2	0	0.9956	5.5901	5.424×10^{-2}
	0.2	0.05	0.998	7.1451	5.424×10^{-2}
	0.2	0.1	1.000	5.503	5.233×10^{-2}
	0.2	0.15	1.002	6.6786	5.148×10^{-2}
	0.2	0.2	1.0043	6.4763	5.069×10^{-2}
	1.0	0	1.0488	4.6764	3.585×10^{-2}
	1.0	0.25	1.0512	4.6382	3.517×10^{-2}
	1.0	0.5	1.0534	4.6024	3.455×10^{-2}
	1.0	0.75	1.0554	4.5686	3.399×10^{-2}
	1.0	1.0	1.0573	4.5366	3.346×10^{-2}
	10	0	1.1106	4.2156	2.389×10^{-2}
	10	2.5	1.1122	4.3203	2.399×10^{-2}
	10	5.0	1.1136	4.4518	2.409×10^{-2}
	10	7.5	1.1149	4.6173	2.421×10^{-2}
	10	10.0	1.1162	4.8276	2.433×10^{-2}
	15	0	1.1194	5.7663	2.468×10^{-2}
	15	3.75	1.1212	6.7666	2.49×10^{-2}
	15	7.5	1.1229	8.3905	2.513×10^{-2}
	15	11.25	1.1246	10.636	2.538×10^{-2}
	15	15.0	1.126	13.194	2.564×10^{-2}
H_2O	0.2	0	0.859	6.1383	9.267×10^{-2}
	0.2	0.05	0.8881	5.9935	6.822×10^{-2}
	0.2	0.1	0.9141	5.5642	5.808×10^{-2}
	0.2	0.15	0.9341	5.198	5.218×10^{-2}
	0.2	0.2	0.9502	4.895	4.817×10^{-2}
	1	0	0.9883	4.1752	4.95×10^{-2}
	1	0.25	1.0226	3.5598	4.504×10^{-2}
	1	0.5	1.0460	3.123	3.393×10^{-2}
	1	0.75	1.0622	2.8148	3.147×10^{-2}
	1	1.0	1.0736	2.5878	3.012×10^{-2}
	10	0	1.1205	1.5392	2.937×10^{-2}
	10	2.5	1.1045	1.0858	3.372×10^{-2}
	10	5.0	1.1005	0.7808	3.456×10^{-2}
	10	7.5	1.0985	0.6092	3.498×10^{-2}
	10	10.0	1.0974	0.4994	3.522×10^{-2}
	100	0	1.1224	0.1733	3.229×10^{-2}
	100	25	1.1059	0.1076	3.433×10^{-2}
	100	50	1.1012	0.0777	3.490×10^{-2}
	100	75	1.0989	0.0608	3.517×10^{-2}
	100	100	1.0976	0.0499	3.533×10^{-2}

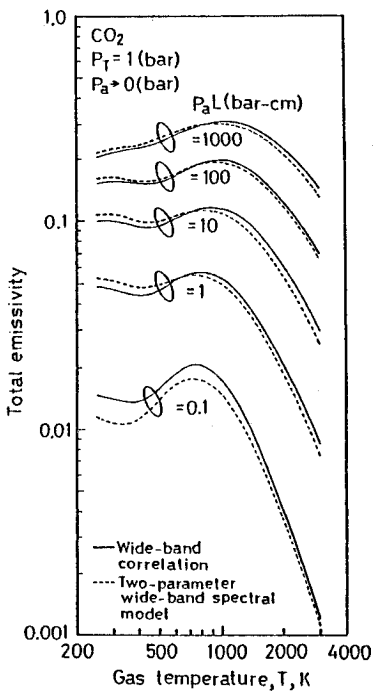

Fig. 1 Total emissivity of carbon dioxide at a total pressure of 1 bar and 0 partial pressure.

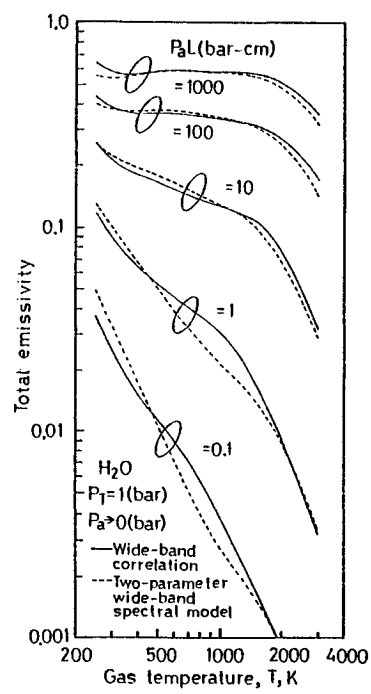

Fig. 2 Total emissivity of water vapor at a total pressure of 1 bar and 0 partial pressure.

Table 2 Approximate expressions of K_1 and K_2 for $0.2 \le P_T \le 100$ bar

	K_1	K_2
CO_2	$K_1 = a_0(P_T) + a_1(P_T)x$	$K_2 = b_0(P_T) + b_1(P_T)x$
	$a_0(P_T) = 1.21106 - \dfrac{0.5089727}{1 + 2.137272P_T^{0.2814413}}$	$b_0(P_T) = 3.62321(P_T/10)^{-0.111936}$ $(P_T < 4.72$ bar$)$
		$= 0.5 \exp\left[\sum_{n=0}^{3} c_n(P_T/10)^n\right]$ $(P_T \ge 4.72$ bar$)$
		$c_0 = 2.032745$, $c_1 = 0.2009378$
		$c_2 = -0.439998$, $c_3 = 0.333206$
	$a_1(P_T) = \dfrac{0.01126122}{1 + 0.3772231P_T^{0.4469997}}$	$b_1(P_T) = 0.5 \sum_{n=0}^{5} d_n(P_T/10)^n$
		$d_0 = -0.4030279$, $d_1 = 1.693137$
		$d_2 = -7.537328$, $d_3 = 2.091479 \times 10$
		$d_4 = -2.421177 \times 10$, $d_5 = 1.077053 \times 10$
H_2O	$K_1 = a_0(P_T) + a_1(P_T)x$	$K_2 = b_0(P_T) + b_1(P_T)x + b_2(P_T)x^2$
	$a_0(P_T) = 1.122405 - \dfrac{0.313022}{1 + 1.550566P_T^{1.220443}}$	$b_0(P_T) = 0.5 \exp\left[\sum_{n=0}^{8} c_n(\sqrt{P_T})^n\right]$
		$c_0 = 2.126875$, $c_1 = -3.41882 \times 10^{-1}$
		$c_2 = -7.164437 \times 10^{-2}$, $c_3 = 3.080315 \times 10^{-2}$
		$c_4 = 1.162493 \times 10^{-2}$, $c_5 = -1.081961 \times 10^{-2}$
		$c_6 = -6.205409 \times 10^{-4}$, $c_7 = 9.787767 \times 10^{-4}$
		$c_8 = -1.137662 \times 10^{-4}$
	$a_1(P_T) = -0.02304255 + \dfrac{0.1154725}{1 + 0.07313106P_T^{2.616753}}$	$b_1(P_T) = 0.5 \sum_{n=0}^{5} d_n(\sqrt{P_T})^n$
		for $0.2 \le P_T \le 7.599$ bar
		$d_0 = -5.436538$, $d_1 = -2.208452 \times 10^{-1}$
		$d_2 = 1.598175$, $d_3 = -7.490206 \times 10^{-2}$
		$d_4 = -2.302853 \times 10^{-1}$, $d_5 = 0$
		for $7.599 < P_T \le 100$ bar
		$d_0 = -4.355628 \times 10$, $d_1 = 8.39472 \times 10$
		$d_2 = -6.6183 \times 10$, $d_3 = 2.437998 \times 10$
		$d_4 = -4.203552$, $d_5 = 2.749994 \times 10^{-1}$
		$b_2(P_T) = 0.5 \sum_{n=0}^{5} e_n(\sqrt{P_T})^n$
		for $0.2 \le P_T \le 5.04$ bar
		$e_0 = 2.061174$, $e_1 = 5.52477 \times 10^{-1}$
		$e_2 = -1.77187 \times 10^{-1}$, $e_3 = -8.598428 \times 10^{-2}$
		$e_4 = -4.141947 \times 10^{-1}$, $e_5 = 2.978506 \times 10^{-2}$
		$e_6 = 8.341235 \times 10^{-2}$
		for $5.04 < P_T \le 100$ bar
		$e_0 = 5.480294 \times 10$, $e_1 = -1.052001 \times 10^2$
		$e_2 = 7.792057 \times 10$, $e_3 = -2.717683 \times 10$
		$e_4 = 4.496212$, $e_5 = -2.851368 \times 10^{-1}$
		$e_6 = 0$

The Edwards model is defined by Eq. (1) with $K_1 = 1$ and $K_2 \to \infty$, while the modified Edwards model is represented by Eq. (1) with $K_1 = 1$ and $K_2 = 2$. These models, however, involve some defects that need to be improved: e.g., the Edwards model was originally assumed to be only applicable to the overlapped-line case, whereas the modified Edwards model systematically underpredicts the absorption. Recently, the author[4] revised these models by optimally adjusting values of K_1 or K_2 and found that the improved modified Edwards model works comparatively well, even in the nonoverlapped-line region, but, in the overlapped-line region, this model is reduced to the Edwards model with $K_1 = 1$ and is less accurate than the Edwards model with optimally tuned K_1. This result suggests that the two-parameter wideband spectral model in the form of Eq. (1) can be more accurate than the previous ones.

The purpose of this Note is to establish this model for carbon dioxide and water vapor. The two parameters involved in this model are optimally adjusted so as to obtain better agreement between the total emissivity of an isothermal layer of the gas computed directly from its definition and that evaluated from the exponential wideband model for given total and partial pressures. The obtained values of K_1 and K_2 are represented in the form of a polynomial of total and partial pressures. The parameter optimization is made utilizing the Marquard method[5] within a wide range of the gas temperature T_i and the partial pressure-path length product $(P_aL)_j$.

Parameter Optimizations

Optimal values of K_1 and K_2 are determined so that the total emissivity of an isothermal gas layer calculated directly from its definition

$$\varepsilon_s[T_i, (P_aL)_j] = \pi \int_0^\infty \frac{\{1 - \exp[-(P_aL)_j\kappa_\nu/RT_i]\}I_{b\nu}}{\sigma T_i^4}\, d\nu \tag{2}$$

with R being the gas constant agrees well with the total emissivity evaluated from the wideband absorption A_k, i.e.,

$$\varepsilon_w[T_i, (P_aL)_j] = \pi \sum_k A_k I_{b\nu_k}/\sigma T_i^4 \tag{3}$$

$I_{b\nu}$ represents the blackbody intensity at the wave number ν, while $I_{b\nu_k}$ denotes the blackbody intensity at a representative wave number ν_k of a kth band. The objective function $\bar{\sigma}$ is defined by

$$\bar{\sigma} = \sum_{i=1}^{I}\sum_{j=1}^{J}\left\{\frac{\varepsilon_s[T_i, (P_aL)_j] - \varepsilon_w[T_i, (P_aL)_j]}{\varepsilon_w[T_i, (P_aL)_j]}\right\}^2 \tag{4}$$

where the values of K_1 and K_2 are determined by the following conditions:

$$\frac{\partial \bar{\sigma}}{\partial K_1} = 0 \quad \text{and} \quad \frac{\partial \bar{\sigma}}{\partial K_2} = 0 \tag{5}$$

T_i is varied from 250 to 3000 K in increments of 50 K, while $(P_a L)_j$ is assumed to be 0.1, 0.3, 1, 3, 10, 30, 100, 300, or 1000 bar-cm. Thus, $I = 56$ and $J = 9$. The objective function of Eq. (4), which was first utilized by Smith et al.[6] for evaluating coefficients for the weighted sum of a gray gas model, is more appropriate than the objective function based on an absolute error because the optimization is made for the ranges of the gas temperature and the partial pressure-path length product where the total emissivity varies over several orders of magnitude. The bands considered in the calculations are the 15-, 10.4-, 9.4-, 4.3-, 2.7-, and 2.0-μm bands of carbon dioxide and the rotational, 6.3-, 2.7-, 1.87-, and 1.38-μm bands of water vapor. The wideband model parameters are taken from Ref. 7. The optimal values of K_1 and K_2 are determined by varying the total pressure from 0.2 to 100 bar and by changing the partial to total pressure ratio from 0 to 1.

Results and Discussion

Several of the determined values of K_1 and K_2 are shown in Table 1, together with the standard deviation defined by $\sigma^* = \sqrt{\bar{\sigma}/(I \times J)}$. Detailed inspection of Table 1 reveals that, for a given total pressure, the obtained values of K_1 and K_2 can be approximated by a polynomial of the partial to total pressure ratio x, and the resultant expansion coefficients can be expressed as a function of total pressure P_T alone. The obtained approximate expressions are summarized in Table 2. Typical results for the total emissivity computed by making use of the expressions in Table 2 are shown in Figs. 1–4, together with the exponential wideband correlation.

Figure 1 illustrates the total emissivity of carbon dioxide at a total pressure of 1 bar and 0 partial pressure. This figure shows that the present wideband spectral model yields fairly accurate results in predicting the total emissivity. It should be noted that, as seen from Table 1 and also as suggested by Smith et al.,[6] the partial pressure has a negligible effect on the emissivity of carbon dioxide for the considered total pressures. Although Table 1 shows that at $P_T = 15$ bar, the values of K_2 strongly depend on x, the value of $\tanh K_2\eta$ becomes unity under this condition, and therefore, the partial pressure does not affect the absorption. This is generally the case for $P_T > 15$ bar and the value of K_1 is asymptotic to 1.1344 at $P_T \to \infty$.

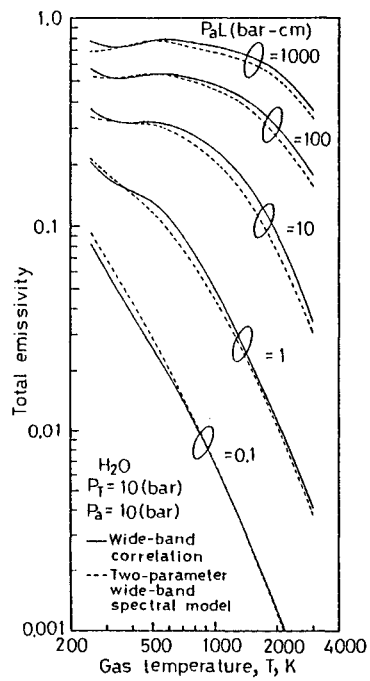

Fig. 3 Total emissivity of water vapor at a total pressure of 10 bar and a partial pressure of 10 bar.

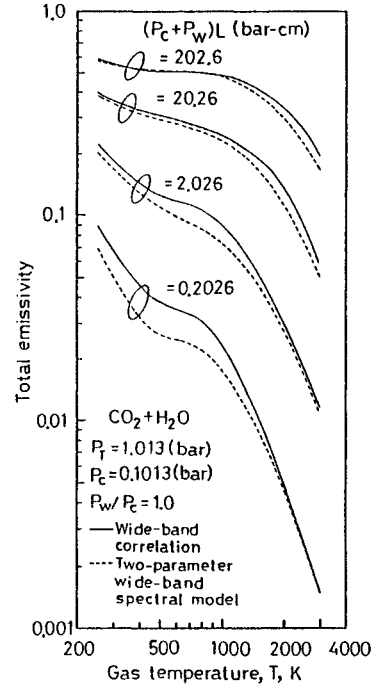

Fig. 4 Total emissivity of carbon dioxide and water vapor mixture. The partial pressures of carbon dioxide and water vapor are 0.1013 bar, while the total pressure is 1.013 bar.

Figure 2 depicts the total emissivity of water vapor at a total pressure of 1 bar and 0 partial pressure, while Fig. 3 indicates the results for the total emissivity of water vapor at a total pressure of 10 bar and a partial pressure of 10 bar. The agreement between the total emissivity computed directly from Eq. (2) and the exponential wideband correlation is satisfactory over the whole region of pressure-path length product.

Finally, Fig. 4 shows the results for the total emissivity of carbon dioxide and water vapor mixture at $P_c = P_w = 0.1013$ bar and $P_T = 1.013$ bar. Here, P_c and P_w denote the partial pressures of carbon dioxide and water vapor, respectively.

Conclusions

The two-parameter wideband spectral model for the absorption coefficients of IR gases has been proposed. The free parameters involved in the model are optimally determined for carbon dioxide and water vapor over the wide range of total and partial pressures, and approximate expressions for the determined values of K_1 and K_2 are obtained. The prediction for the total emissivity by the proposed model agrees well with that by the wideband correlation. The present wideband spectral model is expected to be utilized for solving various radiative transfer problems in real gases or in gas-particle media.

References

[1]Edwards, D. K., Glassen, L. K., Hauser, W. C., and Tuchscher, J. S., "Radiation Heat Transfer in Nonisothermal Nongray Gases," *Journal of Heat Transfer*, Vol. 89, No. 2, 1967, pp. 219–229.

[2]Buckius, R. O., "The Effect of Molecular Gas Absorption on Radiative Heat Transfer with Scattering," *Journal of Heat Transfer*, Vol. 104, No. 4, 1982, pp. 580–586.

[3]Taniguti, H., Kudo, K., Otaka, M., Sumarsono, M., and Obata,

M., "Development of a Monte Carlo Method for Numerical Analysis on Radiative Energy Transfer Through Non-Gray-Gas Layer," *International Journal for Numerical Methods in Engineering*, Vol. 35, 1992, pp. 883–891.

[4]Kamiuto, K., and Tokita, Y., "Wideband Spectral Methods for the Absorption Coefficient of Water Vapor," *Journal of Thermophysics and Heat Transfer*, Vol. 8, No. 4, 1994, pp. 808–810.

[5]Marquard, D. W., "An Algorithm for Least-Squares Estimation of Nonlinear Parameters," *Journal of the Society for Industrial Applied Mathematics*, Vol. 11, No. 2, 1963, pp. 431–441.

[6]Smith, T. F., Shen, Z. F., and Friedman, J. N., "Evaluation of Coefficients for the Weighted Sum of Gray Gases Model," *Journal of Heat Transfer*, Vol. 104, No. 4, 1982, pp. 602–608.

[7]Edwards, D. K., *Advances in Heat Transfer*, Vol. 12, Academic, New York, 1976, pp. 115–193.

Effective Thermal Conductivity of a Saturated Porous Medium

H. E. Imadojemu* and L. H. Porter†
Pennsylvania State University at Harrisburg, Middletown, Pennsylvania 17057-4898

Nomenclature

k = thermal conductivity, W/m K
Q' = heating rate per unit length of wire, W/m
T = temperature, °C
t = time, s
α' = dimensionless heat capacity to normalize the properties of the heated wire
λ = ratio of solid–fluid conductivities k_s/k_f
τ = Fourier's number

Subscripts
eff = effective
f = fluid
s = solid
w = evaluated at the wire
0 = initial condition

Introduction

POROUS material such as sand, crushed rocks, or gravel, with the influence of local pressure difference, migrates and transfers heat energy. This phenomenon can be encountered in the petroleum and geothermal industries. Convection currents in mineral fluids embedded in the Earth crust or convection of heavy fluids in the Earth mantle next to the Earth crust are examples of practical situation in the petroleum industries. In this situation the transport phenomena can be modeled as porous medium and the effective thermal conductivity must be measured in order to correctly predict the convective characteristics of the different grades of the fluids. Heat and mass transfer in porous media also have a wide range of applications in energy storage systems, insulation materials, cores of nuclear reactors, soils, and material handling processes, such as resin transfer molding (RTM) and structural reaction injection molding (SRIM).

A few experimental methods to determine the effective thermal conductivity has been reported in the literature. A review of theoretical models for calculating the effective thermal conductivity of porous medium is provided by Kaviany.[1]

In this investigation, a nonintrusive transient hot wire technique is used to measure the effective thermal conductivity of saturated porous media. We measured the effective thermal conductivity of a porous material saturated in four different fluids and studied the effects of the thermal conductivity of the fluid on the resulting effective conductivity of the porous matrix. Glass beads of 1.0 and 5.0 mm diameter were utilized. Various fluids, such as air, water, engine oil (SAE 30), and ethylene glycol (commercial antifreeze) were used as the saturating fluid.

Experimental Method and Theory

The theory of heat conduction from a line source in an infinite medium will be employed. For large values of τ, and neglecting the contact resistance between the wire and medium, the temperature of the wire is given by Carlslaw and Jaeger[2] as

$$T_w = \frac{Q'}{(4\pi k)}\left\{ln\left(\frac{4\tau}{1.7811}\right) + \left[\frac{(\alpha' - 2)}{2\tau\alpha'}\, ln\left(\frac{4\tau}{1.7811}\right)\right] + \cdots\right\} \quad (1)$$

This applies directly to the needle probe method, but for this investigation, the heated wire will be mounted on an insulating block. The wire and block are placed against the medium being investigated. Perfect insulator assumption means the heat transfer from the wire can only be through the uninsulated-half of its surface. This will cause the wire temperature to rise twice as fast as in the infinite medium case. Thus, the model described by Eq. (1) must be corrected for this experimental approach by multiplying the actual Q' by a factor of 2. For large values of τ that will occur with the passage of time, the model predicts the temperature of the wire will approach an asymptote and increase linearly as a function of the $ln(t)$, as follows:

$$T_w = [Q'/(2\pi k)]\, ln(4\tau/1.7811) \quad (2)$$

It follows that the effective thermal conductivity of the saturated porous medium can be calculated from the slope of this line by

$$k = [Q'/2\pi(T - T_0)]\, ln(t/t_0) \quad (3)$$

The experiments were performed using the apparatus shown in Fig. 1. The probe in this investigation consisted of an insulating mounting foam block (2.5 cm thick, 7 cm wide, and 10 cm long), heated nichrome wire, and thermocouple. The nichrome wire was mounted on one face of the polystyrene foam block to provide a 5-cm-long line source of heat. The

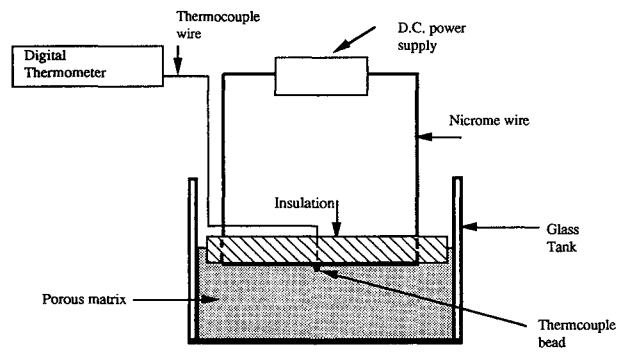

Fig. 1 Experimental layout.

Received July 28, 1994; revision received March 8, 1995; accepted for publication March 14, 1995.

*Assistant Professor, Mechanical Engineering Department.
†Graduate Student.